

# DETECTION OF LOCAL WEATHER EVENTS FROM MULTIWAVELENGTH LIDAR MEASUREMENTS DURING THE EARLI09 CAMPAIGN\*

L. BELEGANTE, C. TALIANU, A. V. NEMUC, D.N. NICOLAE

National Institute of R&D for Optoelectronics, 409 Atomistilor Str., Magurele, Bucharest,  
E-mail: belegantelivio@inoe.inoe.ro,

*Received November 4, 2009*

This paper aims to show the capability of lidar systems to detect atmospheric phenomena taking place within the *Planetary Boundary Layer* (PBL) and the *Free Troposphere* (FT). Usually, lidar systems can measure a variety of atmospheric parameters including aerosols optical and geometrical properties, temperature and wind velocity. Moreover, the *Mixing Layer Height* (MLH), cloud heights, mineral dust and other aerosols layers can be determined from lidar measurements. The Bucharest *Multiwavelength Raman Lidar* (RALI) performed measurements during the *EARlinet Reference Lidars* campaign 2009 – EARLI09. The campaign was organized at the Institute for Tropospheric Physics, in Leipzig, Germany, from May 4<sup>th</sup> to May 29<sup>th</sup>, 2009. One interesting local atmospheric phenomenon related to a frontal passage was observed on RALI *Range Corrected Signal* (RCS) from 26<sup>th</sup> of May 2009. This phenomenon was also confirmed by meteorological observations. Combining Lidar observations with models, we were able to evidence, with a high confidence level, a dust intrusion event and a local extreme weather phenomenon.

*Key words:* multiwavelength lidar, atmospheric phenomena, campaign.

## 1. INTRODUCTION

Atmospheric Lidar systems are laser-based instruments, that emit a beam of light which interacts with the atmosphere. The backscatter radiation is collected using a telescope receiver and then sent to the receiver optics [1]. The description of light interaction with atmospheric constituents (i.e. molecules, particles, clouds) is based on the fundamental theory of electromagnetic wave propagation in various media, well represented in the scientific literature [2,3,4].

Advanced Lidar system with elastic and inelastic channels – such as the Bucharest Multiwavelength Raman Lidar instrument "RALI" – delivers the same time, elastic and inelastic Raman signals, which can be used into the inversion procedure to obtain all optical parameters of the aerosols [5–11].

\* Paper presented at the “Optoelectronic Techniques for Environmental Monitoring” (OTEM-2009), September 30–October 2, 2009, Bucharest, Romania.

Laser remote sensing based systems have the advantage of providing real time vertical aerosol profiles; therefore, lidar systems are suitable instruments for troposphere and even stratosphere studies [12].

Providing a real time response of the atmospheric state, these systems can highlight the evolution of local atmospheric phenomena in the PBL and above.

The EARLI09 campaign was organized at the Institute for Tropospheric Physics, in Leipzig, Germany, from May 4<sup>th</sup> to May 29<sup>th</sup>, 2009. The main objective of EARLI09 was the direct comparison of atmospheric measurements with different lidar systems (reference and non-reference systems). During EARLI09 campaign we had the opportunity to assess the performances of the Bucharest multiwavelength lidar system, to optimize its operation and to test data handling procedures and programs.

The aim of this paper is to emphasize the capability of multiwavelength Raman instruments to detect atmospheric phenomena like dust storms, vortexes, atmospheric turbulences or even storms.

The most common weather phenomena that occur in the troposphere cannot be identified by common ground weather instruments in real time. Due to its high dynamic range and real time response, the lidar system can be used to detect short term, local atmospheric events.

In section 2, named "Data and Methods", we presented the methods used for lidar data processing and models for data analysis. The lidar data analyzed in section 2 have shown a particular case for atmospheric monitoring, using remote sensing techniques, validated with synoptic and meteorological maps. Section 3 is dedicated to results and discussions. The final part of the paper summarizes our conclusions.

## 2. DATA AND METHODS

### 2.1. EARLI09 CAMPAIGN

Figure 1 shows the location and the layout of the systems taking part in EARLI09 campaign. The Bucharest lidar – RALI, was situated on field 1, together with the Potenza, Garmish and the two Munich lidar systems.

During 24 days of measurements, 11 groups from all over Europe, operating 13 lidar systems and a total number of 90 channels, were sounding Leipzig atmosphere on a specified schedule. Whenever the weather permitted, sessions of 3 hours measurements were taken with a 1-minute time resolution. Datasets were used both to assess the performance of the lidar systems involved and to provide analysis of various atmospheric phenomena typical for spring season.



Fig. 1 – Lidar systems at IFT, Leipzig EARLI09 campaign.

RALI, the multiwavelength lidar system of National Institute of R&D for Optoelectronics, was set up, started working and included in EARLINET (European Aerosol Research Lidar Network) in June 2008. This is a state-of-the-art instrument, operating at seven wavelengths and has a maximum of 12 channels. RALI emits at 1064, 532 and 355nm, and receives at 1064, 532p, 532s, 355nm (daytime configuration), and in addition 607, 387, 408nm (nighttime configuration). Most of the channels have both analog and photon counting acquisition, which make possible retrievals up to 15km altitude, depending on the atmospheric conditions. RALI was optimized for the purposes of EARLI09 campaign, so the overlap was reduced to be below 500m and the time resolution was increased to 1 min/profile.

The system is designed to measure continuously, except in case of precipitation or low clouds. In this situation, the lidar signal becomes too strong and the photo-detectors become saturated by the amount of light backscattered from the clouds.

## 2.2. METHODS

Optical parameters of aerosols were extracted from lidar data using RALI pre-processing and processing algorithms [6, 7, 10] based on Fernald-Klett method [8, 9] and *Optical Properties of Aerosols and Clouds* – OPAC software [5]. To determine the height of the PBL and aerosols layers we used an algorithm based on gradient and covariant transform methods [13, 14]. Validation of results obtained from lidar processing algorithm was done either by satellite data or by deterministic models of diagnosis or forecast.

### 2.3. MODELS

Lidar signal retrievals are not direct indicators of aerosol concentration and their microphysical properties, therefore measurements should be correlated with outputs of models and satellite imagery in order to properly assess the origin and type of the detected layers.

Two models were used in this paper: DREAM (*The Dust REgional Atmospheric Model*) forecast model developed by Dr. Slobodan Nickovic [15], running at the Supercomputing Center in Barcelona [16] and HYSPLIT 4 - *Hybrid Single Particle Lagrangian Integrated Trajectory* model [17].

DREAM based on the SKIRON/ETA modeling system and the ETA/NCEP regional atmospheric model, is an integrated modeling system describing the dust cycle in the atmosphere. HYSPLIT is the newest version of a complete system for computing simple air parcel trajectories.

## 3. DISCUSSIONS ABOUT THE LOCAL PHENOMENON OBSERVED ON MAY 26, 2009, LEIPZIG

### 3.1. CASE-STUDY

In this section, we present a case of dust intrusion and a local atmospheric phenomenon occurred during measurements on 26<sup>th</sup> of May 2009. The EARLI09 schedule for this day included daytime measurements, at least 75 minutes, start time 8:00 UTC. The objective of this measurement session was to record a Saharan dust intrusion, forecast by the DREAM model to reach Germany.

A map of the predicted dust load at the time of the Lidar measurements is shown in Fig. 2a. The HYSPLIT air mass backward trajectories analysis (IFT Leipzig starting location: 4 days air mass back trajectories, three levels: 2500m, 3500m, 4500 m for 26<sup>th</sup> of May 2009 at 00:00 UTC) is shown in Fig. 2b. Both models indicated north-west Sahara as the origin of the air masses.

Lidar measurements performed on the previous day indicated a dust layer at 4500m in a clear atmosphere. On May 26<sup>th</sup>, cloud coverage was 20% (06 UTC) and reaching 60% at 12 UTC as it also can be seen from the map of precipitation forecasted by DREAM (fig 2a, insert panel). We assumed that, aerosols (Saharan dust) were involved in condensation processes and consequently in clouds' development. The rain during the previous night confirms this idea. This cycle – aerosol intrusion + cloud formation+ precipitation- is a common process, but very rare involves storms and extreme weather events. During the day of May 26<sup>th</sup>, a short-duration thunderstorm had developed in the *Planetary Boundary Layer* (PBL) and reached the *Free Troposphere* (FT), overlapping the dust intrusion event. This mix of the two phenomena was recorded by our lidar system. *The Range Corrected Signal* (RCS) time series for more than 2 hours during May 26, 2009 are shown in Figs. 3 a, b, c, d.

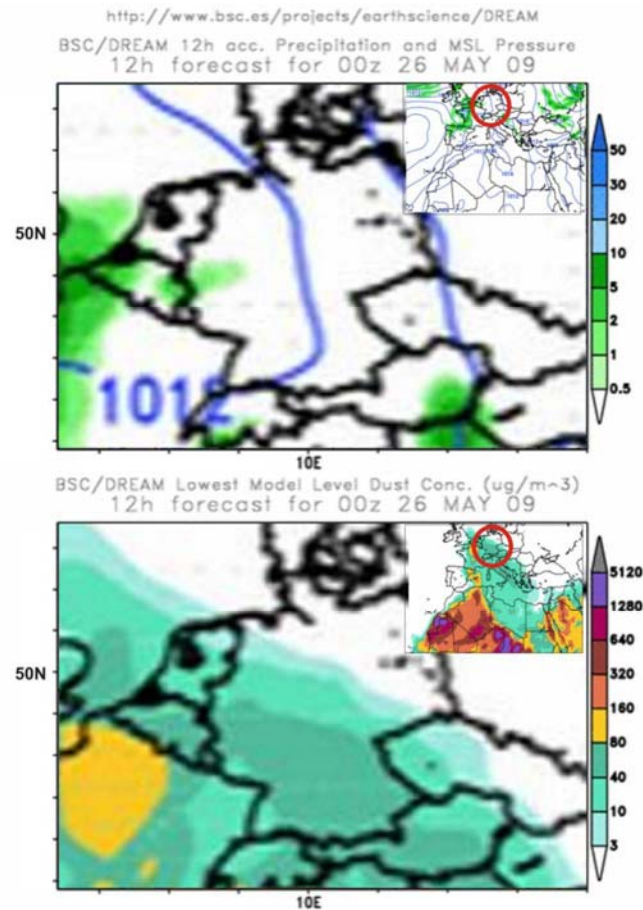


Fig. 2a – Map of precipitation (upper panel) and Saharan dust concentration (lower panel) forecasted by DREAM for 26 May 2009 at 00:00 UTC.

Even though the transition between the PBL and FT is not visible in the RCS due to high turbulence of the atmosphere [18], the gradient at 2000–4500m indicates the presence of dust from long-range transport. The gradient method have been applied to the RCS [14] in order to identify strong variations in lidar signal and therefore layers with different optical properties (Fig. 3b)

The RCS image clearly have shown the presence of an aerosol layer between 2000–4500 m altitude that persisted during the time of the measurements (Figs. 3a, c, d). In addition, on RCS image an undefined local and deep convective cloud was detected. This spectacular cloud had a short life and we assumed that it was associated to the instability behind the cold front (Figs. 4a, b), which passed in previous hours. In addition, the presence of advected tropical air mass (Fig.2b and figs 5a, b) loaded with aerosol explains the appearance of this phenomenon.

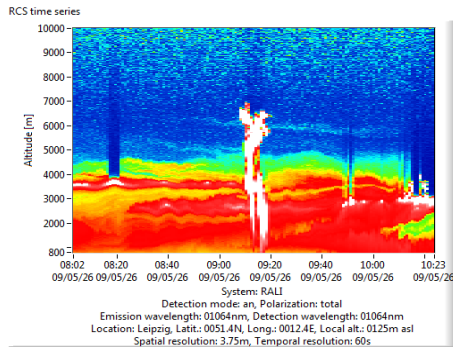


Fig. 3a – Range Corrected Signal time series from lidar (1064nm), May 26<sup>th</sup>, 2009, Leipzig.

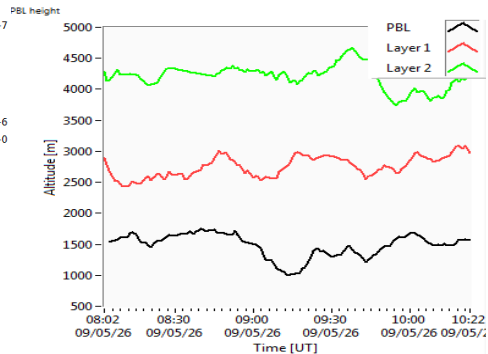


Fig. 3b – Atmospheric layers obtained from RALI RCS, May 26<sup>th</sup>, 2009, Leipzig.

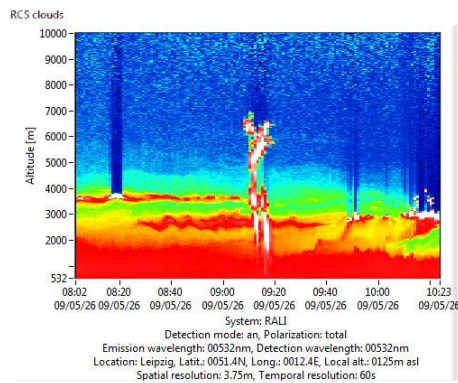


Fig. 3c – Range Corrected Signal time series from lidar (532nm), May 26<sup>th</sup>, 2009, Leipzig.

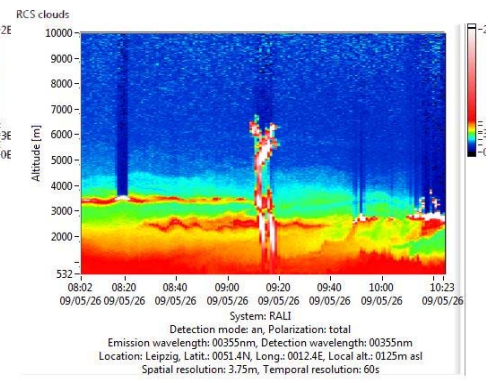


Fig. 3d – Range Corrected Signal time series from lidar (355nm), May 26<sup>th</sup>, 2009, Leipzig.

As can be seen from a comparison between the channels used for measurements on the 26<sup>th</sup> of May 2009 (fig. 3 a, c, d), the cloud formation is more visible on the 1064nm channel than on the 532 and 355 nm. This highlights a size distribution of constituents at around 1  $\mu\text{m}$ . Particles of size equal or greater than 1  $\mu\text{m}$  are specific to cloud droplets and the growth of these droplets is also visible on the 532 and 355 nm channels.

The weather [19] synoptic maps (Fig 4 a,b and Figs 5a,b) reveal the passage of the front and the advection of the tropical air mass (the relative geopotential layer 1000-500 hPa shows warm air mass advection). In addition, the presence of the bridge on altitude shows a south-west air circulation over Germany and very large temperature lapse rates that determined wind enhancements.

Comparative analysis of the geo-potential fields and particle trajectories suggest a mass mixing process during this day.

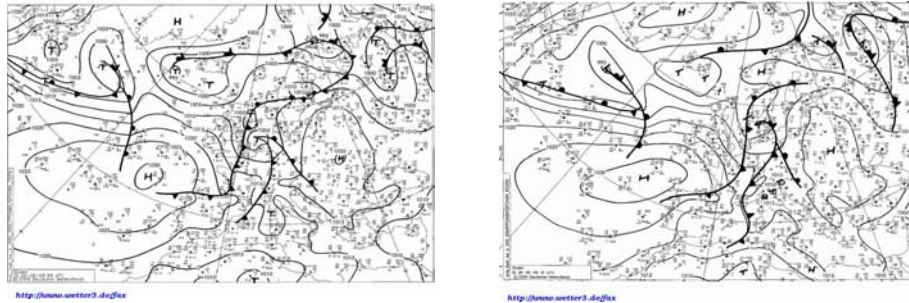


Fig. 4 a,b – Synoptic maps May 26<sup>th</sup>, 2009 (06 UTC left and 12 UTC right).

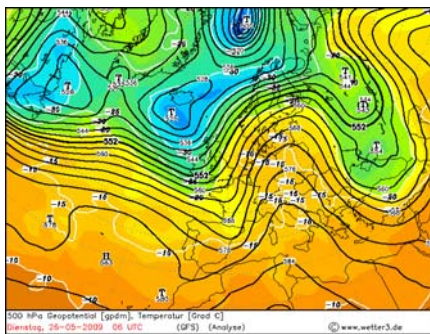


Fig. 5a – 500hPa map of geopotential and mean temperature for 26 May 2009 at 06:00 UTC.

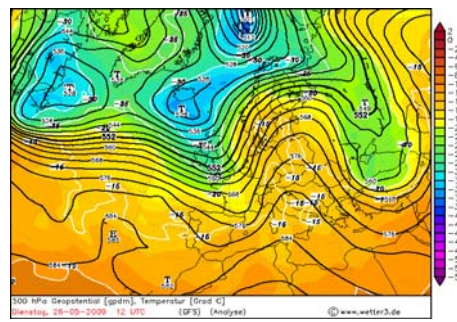


Fig. 5b – 500hPa map of geopotential and mean temperature for 26 May 2009 at 12:00 UTC.

The READY GDAS (Real Time Environmental Applications and Display System - Global Data *Assimilation System*) [16] Meteorological data for 26 May 2009 (Fig 6a – 6c) show main meteorological parameters, pointing out high instability of the atmosphere and large temporal and vertical gradients of humidity and temperature.

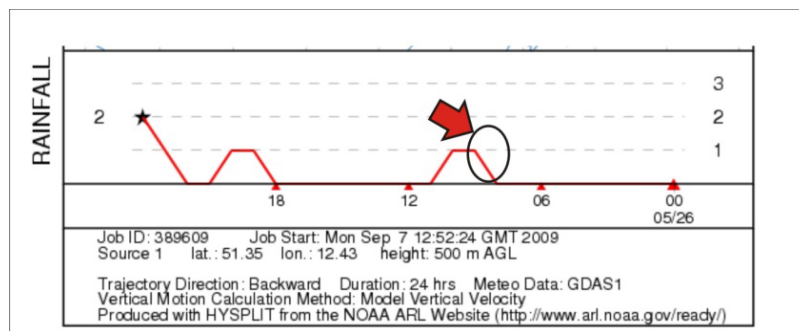


Fig. 6a – READY GDAS Meteorological data for 26 May 2009 – Rainfall, 500m (Above Ground Level) AGL.

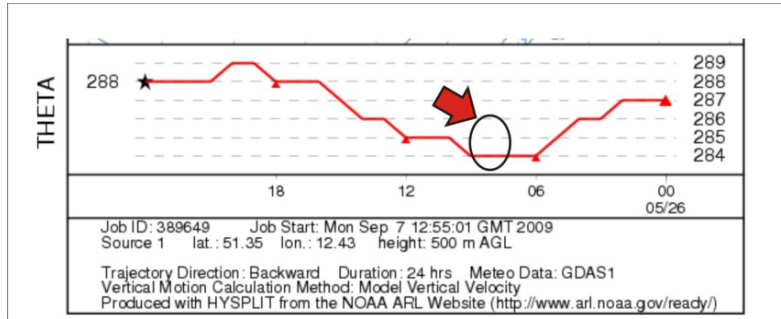


Fig. 6b – READY GDAS Meteorological data for 26 May 2009 – Potential temperature, 500m AGL.

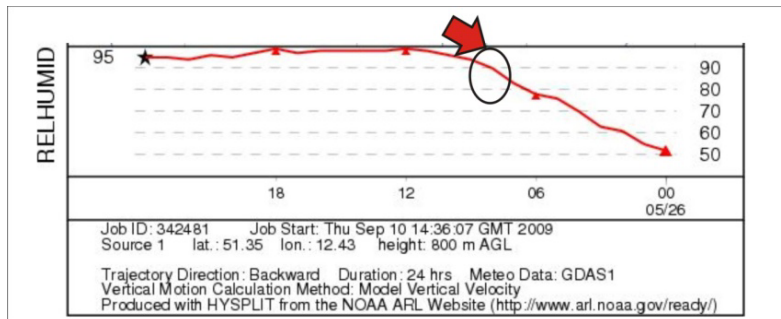


Fig. 6c – READY GDAS Meteorological data for 26 May 2009 – RH, 800m AGL.

One can see that the meteorograms of the potential temperature, the rainfall and the relative humidity have a specific behavior: increase of humidity, decrease of the temperature and sparse local precipitation. These features of the state of the atmosphere lead to the formation of convective clouds and, sometimes with storms.

### 3.2. DISCUSSIONS OF THE RALI DATA

According to DREAM and HYSPLIT models, the aerosol layer at 4000 - 4500m observed by RALI system before the thunderstorm comes from Sahara and passes Mediterranean Sea and France in its way to Germany.

From analysis of lidar measurements for the period before the thunderstorm, aerosols at 4500m altitude detected over Leipzig (Fig. 7left) have a higher depolarization coefficient (2.2%) than local aerosols within PBL (1.5%) (Fig. 7 right). This fact indicating particles with significant asphericity at that altitude. The color ratio  $\beta_{532}/\beta_{355}$  is  $0.9 \pm 0.1$ ,  $\beta_{1064}/\beta_{532}$  is  $0.7 \pm 0.1$  and Angstrom exponent (355/532) is  $0.1 \pm 0.1$  for this specific layer. These parameters indicate a coarse size distribution around  $1\mu\text{m}$  [13, 17]. On the other hand, the formation of clouds at dust layer altitude indicates that the mineral dust transported from West Sahara to



Europe became hygroscopic upon its arrival due to changes in composition during transport across the Mediterranean Sea. The hygroscopic nature of the aged mineral dust increases its ability to nucleate cloud droplets (i.e., act as cloud condensation nuclei) and favors cloud development [14].

RCS time series show cloud formation but also an unexpected thunderstorm with the origin inside PBL and developing high backscatter on the vertical up to 7km.

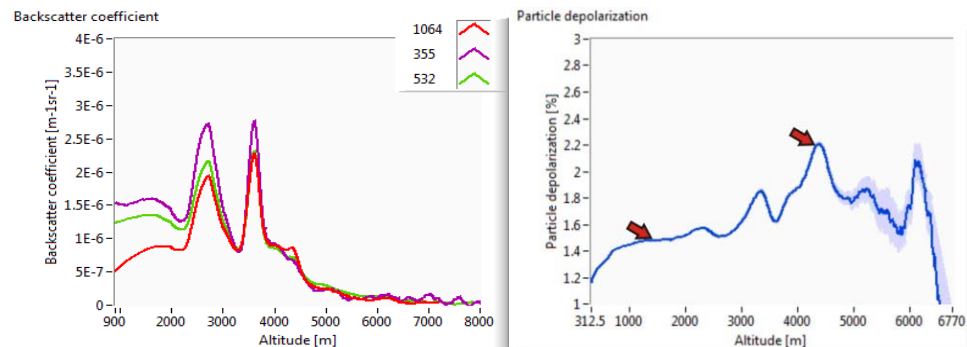


Fig. 7 – Backscatter profiles (left) and particle depolarization profile (right).

Microphysical characteristics of dust and mixed aerosols alone do not explain the evolution of this phenomenon. Moreover, due to limitation of Mie algorithm, proper values for the backscatter and depolarization coefficient cannot be obtained if cloud particles are present at low altitudes. More likely, this local phenomenon can be explained by the instability in air mass over Leipzig.

The campaign site, situated in Leipzig is a suitable place for this type of phenomena occurrence due to the orography of the area.

#### 4. CONCLUSIONS

This study underline the capability of a complex multiwavelength Lidar system to highlight events such as atmospheric turbulence of air in the troposphere, while other regular meteorological instruments are not able.

Combining multi-wavelength Lidar data processing program with DREAM and HYSPLIT models, we were able to evidence, with a high confidence level, a dust intrusion event and a local extreme weather phenomena.

In synergy with lidar retrievals from 26<sup>th</sup> of May 2009, the READY GDAS meteorological data confirmed that the weather conditions for that day were favorable for atmospheric events such as the one observed by the Bucharest Raman Lidar System.

Considering the complexity of information necessary for a complete understanding of processes in the atmosphere, no instrumentation proved to be capable so far to provide reasonable answers. Only a synergy of ground-based, airborne and remote sensing instruments, as well as regional and global atmospheric models could provide this.

*Acknowledgments.* The authors wish to acknowledge Norway Grants for RADO contract STVES 115266, European Commission for DELICE grant FP7 REGPOT-2008-1 229907 and EARLINET-ASOS project (EU Coordination Action, contract n° 025991 (RICA)). The authors express gratitude to the NOAA Air Resources Laboratory (ARL) for the HYSPLIT air mass trajectories model.

#### REFERENCES

1. Measures R.M., *Laser Remote Sensing. Fundamentals and Applications*, Krieger Publishing Company, Malabar, Florida, 1992.
2. Mie G., *Ann. Physik* **25**, 377–445 (1908).
3. Mishchenko M.I., Hovenier J.W., Travis L.D., *Light Scattering by Nonspherical Particles. Theory, Measurements, and Applications*, Academic Press, San Diego, p. 152–157, 2000.
4. Brechtel F. J., Kreidenweis S.M. and Swan H. B., Air mass characteristics, aerosol particle number concentrations, and number size distributions at Macquarie Island during the First Aerosol Characterization Experiment (ACE 1), *J. Geophysical Res.*, **103**, 16351–16367, 1998.
5. Hess M., Koepke P., Schult I., *Optical properties of aerosols and clouds: the software package OPAC*, *Bull. Amer. Meteor. Soc.*, **79**, pp. 831–844, 1998.
6. Camelia Talianu, Doina Nicolae, Jeni Ciuciu, Anca Nemuc, E. Carstea, L. Belegante, M. Ciobanu, *New Algorithm For The Retrieval Of Aerosol's Optical Parameters By Lidar Data Inversion*, ECMI Series Vol. 11, Springer,, pp. 55–62, 2007.
7. C. Talianu, D. Nicolae, J. Ciuciu, M. Ciobanu, V. Babin, Planetary boundary layer height detection from LIDAR measurements, *J. Optoelectron. Adv. Mater.*, vol. 8, no. 1, pp. 243–246, 2006.
8. Fernald F.G., Herman B.M., and Reagan J.A., *Determination Of Aerosol Height Distribution By Lidar*, *J. Appl. Meteorol.* **11**, 482–489, 1972.
9. Klett J.D., *Stable Analytical Inversion Solution For Processing Lidar Returns*, *Appl. Opt.* **20**, 211–220, 1981.
10. D. Nicolae, C.P. Cristescu, Laser remote sensing of tropospheric aerosol, *J. Optoelectron. Adv. Mater.*, vol. 8, no. 5, p.1781-1795, 2006.
11. D. Nicolae, C. Talianu, R.-E. Mamouri, E. Carstea, A. Papayannis, G. Tsaknakis, Air mass modification processes over the Balkans area detected by aerosol Lidar techniques, *J. Optoelectron. Adv. Mat. – Rapid communications* Vol. 2, No. 6, p. 405–412, 2008.
12. D. Nicolae, C. Talianu, V. Babin, L. Belegante, Benefits and drawbacks of laser remote sensing in atmosphere science, *U.P.B. Sci. Bull.*, Series A, Vol. 70, No. 4, ISSN 1454-2331, pp. 5–14, 2008.
13. Brooks, Ian M. Finding boundary layer top: Application of a wavelet covariance transform to Lidar Backscatter Profiles. *J. of Atmos. and Oceanic Technol.*, **20**, 1092–1105, 2003.
14. Sabina Stefan, Doina Nicolae and Mihaela Caian: Atmospheric aerosol secrets in lasers light ( in Romanian language) Ed. Ars Docendi, Bucuresti 2008, ISBN 978-973-558-357-6.
15. Nickovic, S., A. Papadopoulos, O. Kakaliagou and G. Kallos, *Model for prediction of desert dust cycle in the atmosphere*, *J. Geophys. Res.*, **106**, pp. 18113–18129, 2001.

16. <http://www.bsc.es/projects/earthscience/DREAM/>.
17. [http://www.arl.noaa.gov/ready/hysp\\_info.html](http://www.arl.noaa.gov/ready/hysp_info.html).
18. Dynamic of the lower troposphere from mutiwavelength LIDAR measurements, Anca Nemuc, Doina Nicolae, Camelia Talianu, Emil Carstea, Cristian Radu, *Romanian Reports in Physics*, Vol. 61, No. 2, 2009.
19. <http://www.wetter3.de/Archiv/>.
20. Papayannis A. et al., Two years of continuous observations of Saharan dust events over the European continent using a coordinated lidar Network in the frame of the EARLINET Project, in Lidar Remote Sensing in Atmospheric and Earth Sciences, 309–312, *21<sup>th</sup> International Laser Radar Conference, Quebec, Canada*, 2002.
21. Müller D., Ansmann A., Mattis I., Tesche M., Wandinger U., Althausen D., Pisani, G., Aerosol-type-dependent lidar ratioobserved with Raman lidar. *J. Geophys. Res.*, 112, 2006JD008292, 2007.